

# Influence of Zirconium Substitution on the Chemical Stability and Conductivity of BaCeO<sub>3</sub>-based Proton Conductors

Kwang Hyun Ryu, Sossina M. Haile, Geoff Staneff and Sangita Jamindar  
Materials Science, 138-78, California Institute of Technology  
1200 California Blvd, Pasadena, CA 91125

Doped barium cerate is a well-known proton conducting oxide. Introduction of a trivalent dopant onto the quadrivalent cerium site results in the creation of oxygen vacancies. Upon exposure of the material to humid atmospheres the compound dissolves OH groups onto the formerly vacant oxygen sites and additional protons are incorporated at other oxygen ion sites. Protons present in the form of hydroxyl ions can easily jump from one oxygen ion to the next, giving rise to the observed high proton conductivity. Barium cerate has been proposed as a fuel cell electrolyte, offering high conductivity at temperatures lower than those currently utilized in zirconia based solid oxide fuel cells. It has been observed, however, that exposure to CO<sub>2</sub> containing atmospheres, as would be present in the fuel cell environment, causes degradation of the material as it reacts to form barium carbonate and cerium oxide. In contrast to barium cerate, barium zirconate is quite stable in CO<sub>2</sub> containing atmospheres, but is undesirable for applications because of its relatively low proton conductivity.

In the present work, the conductivity and chemical stability of doped barium cerate have been investigated as a function of zirconium substitution onto the cerium site. Compounds in the system BaCe<sub>0.9-x</sub>Zr<sub>x</sub>M<sub>0.1</sub>O<sub>3-δ</sub>, where M is Gd, Nd or Yb, were prepared by solid state reaction. In order to investigate the role of processing route and chemical homogeneity on the properties, two synthesis routes were pursued. In the first case, appropriate quantities of BaCO<sub>3</sub>, CeO<sub>2</sub>, ZrO<sub>2</sub> and M<sub>2</sub>O<sub>3</sub> were directly calcined at temperatures between 1400 and 1600°C. In the second case, a homogeneous solution of CeO<sub>2</sub>, ZrO<sub>2</sub> and M<sub>2</sub>O<sub>3</sub> was first prepared by calcination at a high temperature (1500°C) to which BaCO<sub>3</sub> was subsequently added and the milled powders calcined at a temperature of 1350°C. The final calcination step was carried out at this relatively low temperature in order to minimize evaporative loss of BaO from the material. Calcined powders were characterized by X-ray powder diffraction and transmission electron microscopy. Thermal gravimetric analysis (TGA) and differential thermal analysis (DTA) were performed in flowing CO<sub>2</sub> to assess chemical stability. The conductivity of sintered pellets (density greater than 95% of theoretical) was measured by A.C. impedance spectroscopy (HP 4292A, 20Hz to 1 MHz) over a wide temperature range in both dry and H<sub>2</sub>O-saturated argon. Sputtered platinum served as the electrode material.

X-ray diffraction analysis demonstrated that, as expected, the unit cell parameter decreases monotonically with increasing Zr content. Transmission electron microscopy revealed that samples calcined at 1400° and 1500°C (first synthesis route) contained inclusions of unreacted CeO<sub>2</sub>, despite the absence of peaks attributable to this material in the X-ray powder diffraction patterns. No such inclusions were present in the materials calcined at 1600°C, or in those materials prepared by the second synthesis route.

The reactivity of BaCe<sub>0.9-x</sub>Zr<sub>x</sub>M<sub>0.1</sub>O<sub>3-δ</sub> decreased with increasing Zr content, as anticipated, and as is evident from Fig. 1, in which the thermal behaviors of BaCe<sub>0.9</sub>Nd<sub>0.1</sub>O<sub>3</sub> and BaCe<sub>0.7</sub>Zr<sub>0.2</sub>Nd<sub>0.1</sub>O<sub>3-δ</sub> are compared. The material containing no Zr, BaCe<sub>0.9</sub>Nd<sub>0.1</sub>O<sub>3</sub>, showed a gradual weight gain above 600°C, Fig 2(a), due to reaction with CO<sub>2</sub>. Further heating induced weight loss at ~1130° which was accompanied by a sharp peak in the DTA curve at ~ 1150°C. During subsequent cooling, the material remained stable to a temperature of ~1000°C, at which point it again reacted with CO<sub>2</sub>, as evidenced by an increase in weight. A peak in the DTA curve accompanied this reaction as well. The endothermic peak at ~ 750°C (noted on cooling) likely resulted from a structural transition of BaCO<sub>3</sub> from its

rhombohedral to orthorhombic form. The Gd and Yb doped materials exhibited similar behavior, although the extent of the reaction with  $\text{CO}_2$

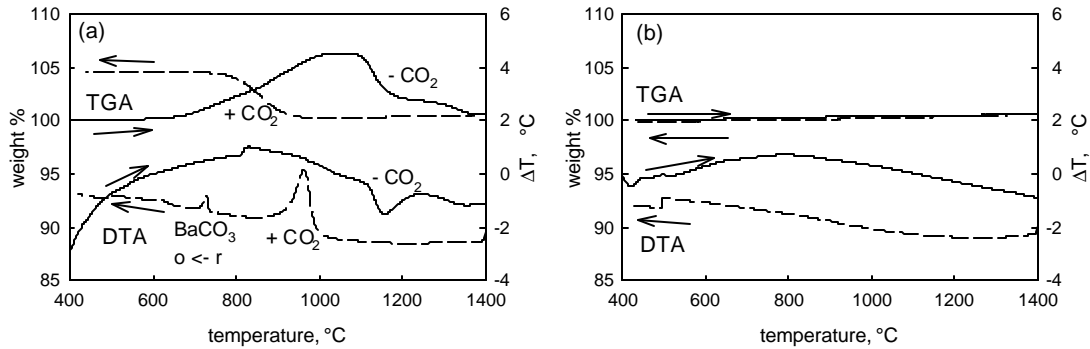


**Fig. 1.** TGA and DTA traces of  $\text{BaCe}_{0.9-x}\text{Zr}_x\text{Nd}_{0.1}\text{O}_3$  in flowing  $\text{CO}_2$ : (a)  $\text{BaCe}_{0.9}\text{Nd}_{0.1}\text{O}_3$ , (b)  $\text{BaCe}_{0.7}\text{Zr}_{0.2}\text{Nd}_{0.1}\text{O}_3$ .

differed for each of the dopants. The results of the thermal analysis experiments are summarized in Fig. 2, in which the maximum mole per cent of barium to react with  $\text{CO}_2$  is plotted (a) as a function of Zr content for each of the three dopants (samples calcined at  $1500^\circ\text{C}$ ), and (b) as a function of calcination temperature for the compositions  $\text{BaCe}_{0.7}\text{Zr}_{0.2}\text{Gd}_{0.1}\text{O}_{3-\delta}$  and  $\text{BaCe}_{0.8}\text{Zr}_{0.1}\text{Nd}_{0.1}\text{O}_{3-\delta}$ . The enhanced stability with increased calcination temperature is likely due to the increased homogeneity of the samples, but may also be in part due to BaO loss. It is evident that the different dopant ions lead to significant differences in reactivity, despite their chemical similarity. Moreover, the extent of enhancement of the chemical stability by the introduction of Zr into  $\text{BaCeO}_3$  is significantly greater than one calculates from a simple solid solution model, based on the known reactivities of  $\text{BaCeO}_3$  and  $\text{BaZrO}_3$  individually with  $\text{CO}_2$ .

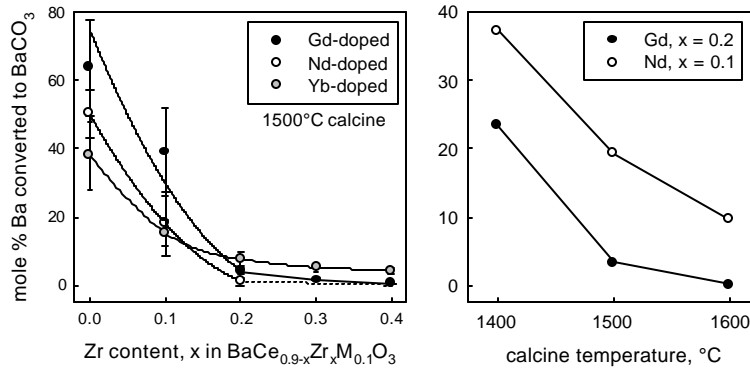


**Fig. 2** Reactivity of perovskite as a function of (a) Zr content; (b) calcine T

The (bulk) conductivities of Nd and Gd doped samples are shown in Fig. 3. A.C. impedance plots revealed the presence of two arcs in the Nyquist representation, and the high frequency arc was attributed to bulk transport processes. In addition, because the measurements were performed at low temperatures ( $100\text{--}450^\circ\text{C}$ ), the entirety of the conductivity was taken to be due to protons. It is evident that the conductivity decreased monotonically with increasing Zr content. A similar result was obtained for the grain boundary conductivity. Moreover, the activation energy for proton transport increased monotonically with Zr content, whereas the pre-exponential term remained relatively insensitive to this parameter. Despite the decrease in conductivity, there appears to be a composition window centered about

$\text{BaCe}_{0.7}\text{Zr}_{0.2}\text{Nd}_{0.1}\text{O}_{3-\delta}$  at which both the chemical stability and proton conductivity are sufficiently high to meet the requirements of fuel cell applications.

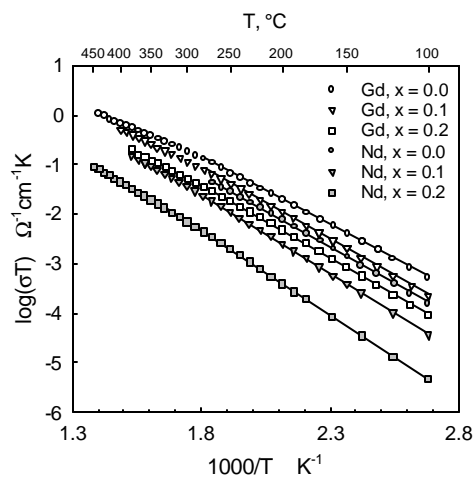


**Fig. 3** Conductivity of  $\text{BaCe}_{0.9-x}\text{Zr}_x\text{M}_{0.1}\text{O}_{3-\delta}$  in  $\text{H}_2\text{O}/\text{argon}$